

Intrinsic tunneling in phase separated manganites

G. Singh Bhalla, S. Selcuk, T. Dhakal, A. Biswas, A. F. Hebard*
Department of Physics, University of Florida, Gainesville FL 32611

We present evidence of direct electron tunneling across intrinsic insulating regions in sub-micrometer wide bridges of the phase separated ferromagnet $(\text{La,Pr,Ca})\text{MnO}_3$. Upon cooling below the Curie temperature, a predominantly ferromagnetic supercooled state persists where tunneling across the intrinsic tunnel barriers (ITBs) results in metastable, temperature-independent, high-resistance plateaus over a large range of temperatures. Upon application of a magnetic field, our data reveal that the ITBs are extinguished resulting in sharp, colossal, low-field resistance drops. Our results compare well to theoretical predictions of magnetic domain walls coinciding with the intrinsic insulating phase.

PACS numbers: 75.47.Lx, 75.60.Ch, 71.30.+h

In ferromagnetic oxides [1] such as hole-doped manganites, the balancing of electrostatic [2] and elastic [3] energies in addition to competing magnetic interactions may lead to coexisting regions of ferromagnetic metallic (FMM) and insulating phases [4, 5, 6]. Upon reducing the dimensions of such a system, an increase in the easy-axis magnetic anisotropy and a decrease in electrostatic screening [6] can create conditions which favor phase separation at the ferromagnetic domain boundaries resulting in novel insulating stripe domain walls which allow direct electron tunneling [6, 7, 8, 9]. The manganite $(\text{La}_{1-y}\text{Pr}_y)_{1-x}\text{Ca}_x\text{MnO}_3$ provides unique opportunities for exploring the formation of such unique domain walls and intrinsic tunnel barriers (ITBs) due to its well-documented micrometer-scale phase separation into FMM and insulating regions [3, 4]. We present here transport properties of thin $(\text{La}_{0.5}\text{Pr}_{0.5})_{0.67}\text{Ca}_{0.33}\text{MnO}_3$ (LPCMO) films which, when reduced in dimensions, do indeed exhibit the classic signatures of tunneling across ITBs separating adjacent FMM regions. Further, colossal low field magnetoresistance (MR) measurements suggest that the ITBs coincide with ferromagnetic domain walls, implying that the ferromagnetic domain structure in LPCMO is modified.

To clarify the context and implications of our results, we distinguish between experiments that are sensitive to the presence of domain walls coincident with grain boundaries [10, 11] or induced at geometrical constrictions [12, 13, 14], and our experiments, where ITBs [6, 7] result from intrinsic phase separation [3]. In the former category, enhanced low-field magnetoresistance observed in polycrystalline ferromagnetic films of $\text{La}_{0.67}\text{Ca}_{0.33}\text{MnO}_3$ and $\text{La}_{0.67}\text{Sr}_{0.33}\text{MnO}_3$ is attributed to spin-dependent scattering [10] or tunneling [11] across grain boundaries. Low-field magnetoresistance has also been attributed to domain walls artificially induced at microconstrictions in epitaxial $\text{La}_{0.67}\text{Ca}_{0.33}\text{MnO}_3$ films [12] and to domain walls pinned at nanoconstrictions in patterned epitaxial $\text{La}_{0.67}\text{Sr}_{0.33}\text{MnO}_3$ films [13, 14]. Below we show that choosing a system with the appropriate material properties and dimensions can give

rise to highly resistive ITB formation in the absence of mechanical defects.

Calculations incorporating the double exchange model, which also account for electrostatic interactions and screening in phase separated ferromagnets show that narrow stripes of the antiferromagnetic insulating phase (i.e., ITBs) form at magnetic domain boundaries due to enhancement of the easy-axis anisotropy in ultra-thin (2D) manganite films [6]. This results in an abrupt change in magnetization between neighboring FMM domains separated by an ITB, in contrast to classical ferromagnets where the direction of magnetization changes over μm length scales near a domain boundary [15]. The calculations can easily be extended to narrow (1D) geometries such as ours [6]. We choose LPCMO since near the insulator to metal transition temperature, T_{IM} , the FMM phase coexists with insulating phases: the antiferromagnetic charge-ordered insulating [4] (COI) and the paramagnetic charge-disordered insulating phases [16, 17, 18]. Below T_{IM} LPCMO thin films grown on NdGaO_3 are in a predominantly ferromagnetic state [19], making the patterned thin films an ideal system for exploring stripe domain wall and ITB formation. A slight change in the chemistry and doping of the $(\text{La}_{1-y}\text{Pr}_y)_{0.67}\text{Ca}_{0.33}\text{MnO}_3$, ($y = 0.5$) thin films used in this experiment can drastically alter this phase composition [4, 20].

To fabricate our samples, we epitaxially deposited single crystalline, 30 nm thick LPCMO films on heated (820°C) NdGaO_3 (110) substrates using pulsed laser deposition [19]. We first measured (Fig. 1) the temperature-dependent resistance $R(T)$ of several unpatterned LPCMO films before standard photolithography and a manganite wet-etch were used to pattern the films into $2.5 \times 8 \mu\text{m}$ four-terminal bridge structures (see Fig. 1). Measurements were performed on these bridges before they were reduced in width using a focused ion beam as shown in the SEM image in Fig. 1. Care was taken to avoid gallium ion contamination by either directly depositing a polymer followed by a metal (70 nm) or just a metal layer on our structure. Four-terminal resistance measurements were made by sourcing a 1 nA DC

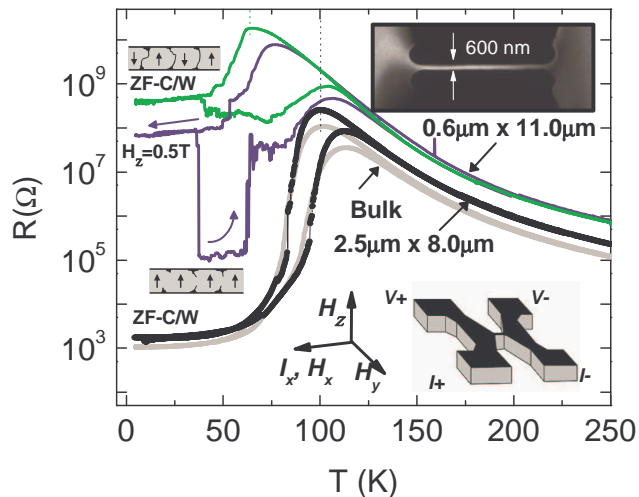


FIG. 1: R vs. T upon zero-field cooling and warming (ZFC/W) of bridges patterned from the same LPCMO film are labeled for the unpatterned film (gray), the $2.5 \mu\text{m} \times 8 \mu\text{m}$ bridge (black) and the $0.6 \mu\text{m} \times 8 \mu\text{m}$ bridge (green) respectively. A FC curve for the $0.6 \mu\text{m} \times 8 \mu\text{m}$ bridge (blue) is also shown. Insulator-metal transitions for the two bridges are indicated by the vertical color-coded dashed lines. Lower inset: schematic of the four-terminal configuration along with the applied field directions. Upper inset: scanning electron micrograph of the $0.6 \mu\text{m}$ wide bridge.

current and measuring the resulting voltages, except for the current-dependent data shown in Figs. 2 and 3.

Figure 1 shows $R(T)$ data for a film patterned into a bridge geometry of $2.5 \mu\text{m}$ width, which is on the order of individual domain length scales [4, 5]. In this case, $R(T)$ emulates unpatterned thin-film behavior (grey) with the exception of small step-like features [23] below the insulator-to-metal percolation transition temperature, $T_{IM} = 100\text{K}$ [21]. However, when the bridge width is reduced to $0.6 \mu\text{m}$, transport is clearly dominated by a few metallic and insulating regions. We attribute the pronounced reduction of T_{IM} to 64K for this narrow bridge to dimensionally-limited percolation (from 2D to nearly 1D). Multiple step-like drops in R occur for $T < T_{IM}$ due to discrete numbers of insulating regions converting to FMM phase. Recent observations of discrete resistivity steps on narrow bridges of other mixed phase manganites also provide evidence of single FMM and insulating regions spanning the full width of the structure [22, 23, 24].

Below $T \approx 50 \text{K}$, the steps in $R(T)$ of the bridge shown in Fig. 1 cease and a nearly temperature-independent resistance in a supercooled state dominates. Though magnetization measurements on unpatterned epitaxial LPCMO thin films confirm a fully ferromagnetic metallic ($3.8\mu_B/\text{Mn}$) state below 50K [19], it is possible that the narrow geometry of the bridge favors the formation of an insulating state. However, the temperature range of approximately 50K over which this high resistance

plateau occurs cannot be explained by such a scenario since any hopping transport associated with the insulating COI phase in LPCMO [20, 25] would show a pronounced resistance increase with decreasing temperature. Additionally, the resistance, $R \approx 5 \times 10^8 \Omega$, of the zero-field-cooled (ZFC) temperature independent plateau is five orders of magnitude larger than the quantum of resistance $h/2e^2 = 12.9 \text{k}\Omega$. By the scaling theory of localization [26] the large resistance value implies that for all dimensions, the $T = 0$ state must be an insulator with infinite resistance, contrary to observation (down to 2K). We therefore conclude that transport across the $0.6 \mu\text{m}$ wide bridge is temperature-independent *direct* tunneling through ITBs comprising atomically thin insulating regions.

Also, unique to the $0.6 \mu\text{m}$ wide bridge is an abrupt colossal (thousandfold) drop in resistance near 40K from the low-temperature field-cooled ($H_z = 5 \text{kOe}$) high-resistance plateau upon field warming (FW) (cf Fig. 1). Similar but relatively small and smooth drops in R are observed in bulk and thin-film LPCMO samples, though the mechanism is unclear [5]. To understand this drop in resistance upon FW, we recall that near T_{IM} in LPCMO the insulating and metallic regions are not pinned but evolve in shape and size with changing temperature [5, 20]. However, below $T_B \approx 40 \text{K}$, the blocking [20] or the supercooling glass transition [27, 28] temperature, the phase separated regions are ‘frozen’ in place [20, 27, 28]. Thus, upon warming up again into the dynamic state above T_B , the phase separated re-

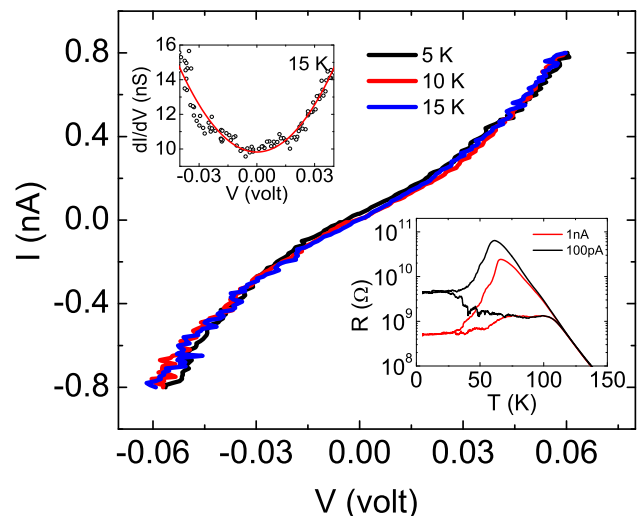


FIG. 2: $I-V$ characteristics for the $0.6 \mu\text{m}$ wide bridge at the three indicated temperatures all measured during one cooling cycle. Top inset: $dI/dV-V$ curve at 15K with a fit (red curve) to the Simmons’ model. Bottom inset: $R(T)$ curves obtained at the indicated currents.

gions and thus the metastable ITBs are no longer frozen in space, possibly giving way field-enhanced FMM conversion of ITBs resulting in a colossal resistance drop.

To confirm that the temperature-independent resistance plateau below $T_B=40$ K (see Fig. 1, main text) is due to ITBs, we measured current-voltage (I - V) curves at 5 K, 10 K, and 15 K as shown in Fig. 2. By numerically differentiating the I - V curve at 15 K, the differential conductance (dI/dV - V) curve shown in the inset of Fig. 2 is obtained. Assuming one ITB in the bridge, the solid red curve was fitted to the data using the equation, $dI/dV = \alpha + 3\gamma V^2$ giving $\alpha = 9.8(1) \times 10^{-9}$ S and $\gamma = 1.0(1) \times 10^{-6}$ S/V². Using Simmons' model[29] and the values for α and γ , we calculate the average barrier height $\bar{\phi}$ to be 0.47 eV and the barrier thickness (t) to be 67 Å. Interestingly, our value for $\bar{\phi}$ is also typical for polycrystalline manganites where tunneling occurs across a single grain boundary (GB) [30, 31]. Unlike GBs however, ITBs are metastable and upon application of a field, bulk resistivity values are recovered in the bridge, confirming the absence of GBs in our structure.

The non-linearity of the I - V curves in Fig. 2 could also be due to current-induced Joule heating. Evidence supporting the absence of Joule heating is shown in Fig. 2, bottom inset, where $R(T)$ is measured at the indicated currents. Here, T_{IM} increases with increasing applied current, in contrast to the behavior found by Sacanell et al. where a decrease in T_{IM} with increasing applied current is attributed to Joule heating [32].

Next, we explore the magnetic properties of ITBs. If the formation of ITBs is linked to the ferromagnetic domain structure of LPCMO, the magnetic field required for the collapse of the ITB will couple to the intrinsic magnetic anisotropy of the thin film. Sensitivity of ITBs to magnetic field direction is verified in Fig. 3a with a subset of the measured field-cooled $R(T)$ traces for the three field orientations (H_x, H_y and H_z) illustrated schematically in Fig. 1. The inset highlights the cooling field directional dependence at 5 K. Here, after a resistance of $10^7 \Omega$ is reached, cooling in a slightly higher field results in an abrupt hundred fold drop in resistance, suggesting a rapid and sudden disappearance of the ITB. Clearly, the in-plane fields H_x and H_y are more effective than H_z in coupling to the magnetization to reach the low resistance FMM state ($R < 10^5$). These observations of anisotropic field-induced ITB extinction show a coupling of the ITBs with the magnetic easy axis which lies within the plane of the film for manganites deposited on (110) NdGaO₃ [1]. The magnetic field values required to reach the low resistance state are on the order of 1 kOe, which though much greater than the measured coercive field in unpatterned films, are not atypical for narrow ferromagnetic wires [33]. The anisotropic MR associated with the ITBs thus suggests that they may indeed coincide with the FMM domain boundaries forming insulating stripe domain walls. The necessity of intrinsic phase separation

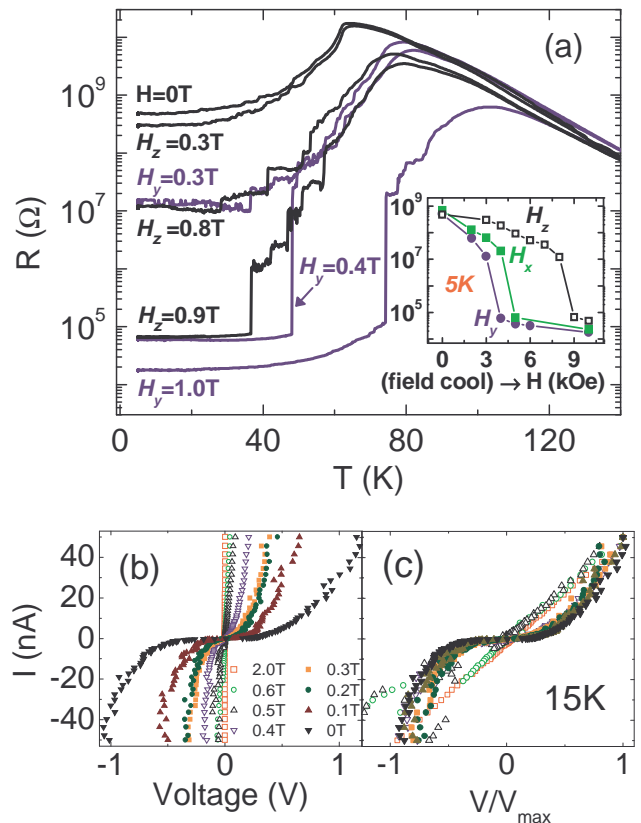


FIG. 3: a) ZFC and FC resistance transitions are labeled by the field directions defined with respect to bridge orientation in Fig. 1. Inset: R measured at 5 K when the bridge is cooled in separate runs at the indicated fields. b) I - V characteristics of the $0.6 \mu\text{m}$ wide bridge zero-field-cooled to 15 K, measured at the indicated values of H_z and (c) normalized to the voltage, V_{max} , measured at maximum applied current.

for stripe domain wall formation is apparent when considering recent measurements of notched bridges on non-phase separated $\text{La}_{0.67}\text{Sr}_{0.33}\text{MnO}_3$ which did not show the presence of highly resistive ITBs [14].

Within the context of stripe domain walls, the MR anisotropy arises when spins in neighboring domains partially align with the field, resulting in reduced spin-dependent scattering at the ITB. The large drop in resistance signifies a conversion of the ITBs to FMM, analogous to field induced extinction of Bloch or Neel domain walls. This notion is confirmed in Fig. 3b where the magnetic field dependence of the I - V curves obtained at 15 K is shown. As H_z increases, the curvature of the I - V curves changes (Fig. 3c). For fields sufficiently large enough to drive the bridge into a low resistance state (≈ 9 kOe in Fig. 3a, inset), the I - V curves become linear (Fig. 3c) suggesting ITB extinction.

The isothermal magnetoresistance curve measured at 57 K in Fig. 4a follows a similar trend with small incremental decreases in resistance followed by a large

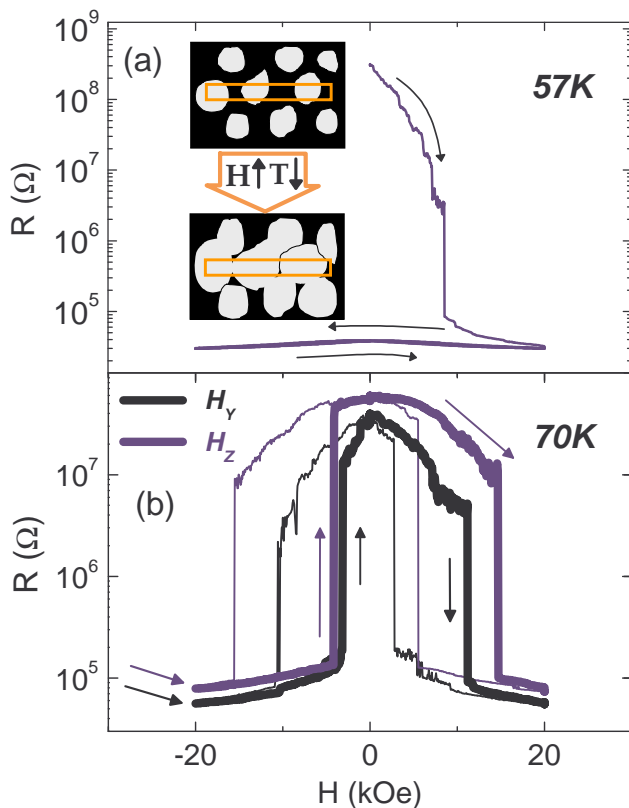


FIG. 4: Field sweeps (H) between ± 20 kOe at temperatures a) $T = 57$ K (below T_{IM}) and b) $T = 70$ K (above T_{IM}) for both increasing (bold curve) and decreasing (thin curve) fields: H_y (black) and H_z (blue). Inset: schematic showing the coalescence of FMM (white) regions at the expense of insulating (black) regions with applied fields or lowering temperatures. The rectangular overlay depicts the $0.6 \mu\text{m}$ bridge.

(hundred fold), irreversible, step-like drop to a low resistance state. Each resistance drop can be explained by either the extinction of an ITB spanning the bridge width, or the incremental conversion of single ITBs to a FMM state. Qualitatively similar R vs. H curves were measured for all $T < T_{IM} = 64$ K. For temperatures $100 \geq T \geq T_{IM} = 64$ K we observe (Fig. 4b) colossal (hundred fold) field-induced resistance changes which unlike for $T < T_{IM}$ occur at well-defined anisotropic switching fields (i.e. the resistance can be switched back to the zero field state upon field removal). At the switching field, there is a reduction in the free energy of the FMM phase and the dominant insulating phase undergoes a first-order phase transition and a concomitant colossal resistance drop [1, 8, 16, 20]. Because the changes in the bridge occur more readily for in-plane (H_y , blue curves) easy-axis fields, we speculate that external field-induced spin alignment between neighboring FMM domains enhances the first order insulator-to-metal transition, just as ITBs are suppressed below T_B when neighboring do-

main spins are aligned (Fig 2). Below 50 K, the inferred resistance-area product [15] (from R vs. H measurements and the zero-field resistance plateau shown in Fig. 1) of a single ITB is $\approx 10^{-5} \Omega\text{m}^2$ [1] or more conservatively, for ten ITBs within the bridge, $\approx 10^{-6} \Omega\text{m}^2$ [1]. These values are 100,000 times greater than the highest value ($10^{-11} \Omega\text{m}^2$) reported for manganites [12, 13, 14].

In summary, we have shown that phase-separation in manganites is strongly modified in confined geometries and leads to the formation of insulating regions thin enough to allow direct electron tunneling, which may also coincide with domain walls separating adjacent FMM domains [6]. Magnetotransport studies of LPCMO bridge structures with submicron widths less than the average size of an FMM region enable us to observe tunneling across these metastable ITBs with record-high resistance-area products. The high resistance of the ITBs, is extremely sensitive to temperature and the magnitude and direction of applied magnetic fields, giving rise to colossal low-field magnetoresistance. In addition to offering rich physical insights into the formation of ferromagnetic domains in phase separated systems, the presence of ITBs introduces new opportunities for manipulating high resistance barriers on the nanometer length scale.

We thank Dmitri Maslov, Pradeep Kumar and Denis Golosov for discussions. This research was supported by the US National Science Foundation under grant numbers DMR-0704240 (AFH) and DMR 0804452 (AB).

* Corresponding author: afh@phys.ufl.edu

- [1] M. Ziese, Rep. Prog. in Phys. **65**, 143 (2002).
- [2] D. I. Golosov, Phys. Rev. B **71**, 014428 (2005).
- [3] K. H. Ahn, T. Lookman, and A. R. Bishop, Nature **428**, 401 (2004).
- [4] M. Uehara, S. Mori, C. H. Chen, and S.-W. Cheong, Nature **399**, 560 (1999).
- [5] L. W. Zhang *et al.*, Science **298**, 805 (2002).
- [6] D. I. Golosov, Phys. Rev. B **67**, 064404 (2003).
- [7] M. S. Rzchowski and R. Joynt, Europhys. Lett. **67**, 287 (2004).
- [8] N. D. Mathur and P. B. Littlewood, Sol. St. Commun. **119**, 271 (2001).
- [9] G. C. Milward, M. J. Calderon and P. B. Littlewood, Nature **433**, 607 (2005).
- [10] A. Gupta *et al.*, Phys. Rev. B **54**, 15629 (1996).
- [11] H. Y. Hwang *et al.*, Phys. Rev. Lett. **77**, 2041 (1996).
- [12] N. D. Mathur *et al.*, J. Appl. Phys. **86**, 6287 (1999).
- [13] J. Wolfman *et al.*, J. of Appl. Phys. **89**, 6955 (2001).
- [14] T. Arnal *et al.*, Phys. Rev. B **75**, 220409 (2007).
- [15] C. H. Marrows, Adv. Phys. **54**, 585 (2005).
- [16] V. Podzorov *et al.*, Phys. Rev. B **64**, 140406 (2001).
- [17] V. Kiryukhin *et al.*, Phys. Rev. B **63**, 024420 (2000).
- [18] H. J. Lee *et al.*, Phys. Rev. B **65**, 115118 (2002).
- [19] T. Dhakal, J. Tosado, and A. Biswas, Phys. Rev. B **75**, 092404 (2007).
- [20] L. Ghivelder and F. Parisi, Phys. Rev. B **71**, 184425

- (2005).
- [21] R. P. Rairigh *et al.*, Nature Physics **3**, 551 (2007).
- [22] T. Wu and J. F. Mitchell, Phys. Rev. B **74**, 214423 (2006).
- [23] H. Y. Zhai *et al.*, Phys. Rev. Lett. **97**, 167201 (2006).
- [24] Y. Yanagisawa *et al.*, Appl. Phys. Lett. **89**, 253121 (2006).
- [25] Y. Z. Xu, D. Ephron, and M. R. Beasley, Phys. Rev. B **52**, 2843 (1995).
- [26] E. Abrahams *et al.*, Phys. Rev. Lett. **42**, 673 (1979).
- [27] P. A. Sharma *et al.*, Phys. Rev. B **71**, 224416 (2005).
- [28] W. D. Wu *et al.*, Nature Materials **5**, 881 (2006).
- [29] J. G. Simmons, J. Appl. Phys. **34**, 1793 (1963).
- [30] W. Westerburg *et al.*, J. Appl. Phys. **86**, 2173 (1999).
- [31] C. Hofener *et al.*, Europhys. Lett. **50**, 681 (2000).
- [32] J. Sacanell, A. G. Leyva, and P. Levy, J. Appl. Physics **98**, 113708 (2005).
- [33] C. Y. Yu *et al.*, Mater. Lett **61**, 1859 (2007).